Neuroscience 254 (2013) 1–17

COMPRESSION INJURY IN THE MOUSE SPINAL CORD ELICITS A SPECIFIC PROLIFERATIVE RESPONSE AND DISTINCT CELL FATE ACQUISITION ALONG ROSTRO-CAUDAL AND DORSO-VENTRAL AXES

A. MCDONOUGH, [a,b] **A.-N. HOANG,** [b] **A. M. MONTERRUBIO,** [a,b] **S. GREENHALGH** [b] **AND V. MARTÍNEZ-CERDEÑO** [a,b]*

[a] *Department of Pathology and Laboratory Medicine, University of California, Davis School of Medicine, 4400 V Street, Sacramento, CA 95817, USA*

[b] *Institute of Pediatric Regenerative Medicine, Shriners Hospitals for Children Northern California, 2425 Stockton Boulevard, Sacramento, CA 95817, USA*

Abstract—Harnessing the regenerative capabilities of endogenous precursor cells in the spinal cord may be a useful tool for clinical treatments aimed at replacing cells lost as a consequence of disease or trauma. To better understand the proliferative properties and differentiation potential of the adult spinal cord after injury, we used a mouse model of compression spinal cord injury (SCI). After injury, adult mice were administered BrdU to label mitotic cells and sacrificed at different time-points for immunohistochemical analysis. Our data show that the rate of proliferation increased in all regions of the spinal cord 1 day after injury, peaked after 3 days, and remained elevated for at least 14 days after injury. Proliferation was greater at the injury epicenter than in rostral and caudal adjacent spinal segments. The number of proliferative cells and rate of proliferation varied between dorsal and ventral regions of the spinal cord and between the gray and white matter. Newly generated cells expressed markers for progenitor cells (Nestin and Olig2), oligodendrocytes (Sox10), astrocytes (S100b and glial fibrillary acidic protein), and microglia (Iba1), but not neuronal markers (Map2 and NeuN). Marker expression varied with regard to the dorso-ventral region, rostro-caudal proximity to the injury epicenter, and time after injury. At early time-points after injury, $BrdU^+$ cells mainly expressed microglial/macrophage and astrocytic markers, while at these same time-points in the control spinal cord the mitotic cells predominately expressed oligodendrocyte and oligodendrocyte progenitor cell markers. The profile of proliferation and cell fate marker expression indicates that after moderate compression, the spinal cord has the capacity to generate a variety of glial cells but not neurons, and that this pattern is space and time specific. Future studies should focus on ways to control proliferation and cell fate after injury to aid the development of cell replacement treatments for SCI.

Key words: spinal cord injury, precursor cells, proliferation, cell fate.

INTRODUCTION

After spinal cord injury (SCI), a process of neuronal and glial cell death begins immediately (Grossman et al., 2001). This process also induces the release of cytokines, growth factors, and cytotoxic amino acids (Zai et al., 2005; Eftekharpour et al., 2008; Ruff et al., 2008), resulting in further cell death and damage. The consequences of SCI include impairments in sensation and motor function and a host of clinical complications (Hawryluk et al., 2008). Despite the initial degenerative responses, the mammalian spinal cord is capable of some repair through endogenous mechanisms such as axonal sprouting (Weidner et al., 2001; Menet et al., 2003; Fouad et al., 2004; Liebscher et al., 2005; Gensel et al., 2006; Okano et al., 2007) and proliferation of precursor cells (Vaquero et al., 1981, 1987; Johansson et al., 1999; Namiki and Tator, 1999; Horner et al., 2000; McTigue et al., 2001; Takahashi et al., 2003; Mothe and Tator, 2005; Zai et al., 2005; Zai and Wrathall, 2005; Horky et al., 2006; Lytle and Wrathall, 2007; Meletis et al., 2008; Sellers et al., 2009; Barnabe-Heider et al., 2010).

Previous studies reported the existence of ependymal cell proliferation after SCI (Vaquero et al., 1981, 1987; Beattie et al., 1997; Mothe and Tator, 2005; Meletis et al., 2008; Barnabe-Heider et al., 2010). More recent studies have focused on proliferation within other regions of the spinal cord, particularly the subpial white matter (Horner et al., 2000; Petit et al., 2011). As there may be two, or more, populations of cells responding to injury, the precise identity and niche of precursor cells remain unclear. We know that glial progenitor cells, which proliferate in both intact and injured spinal cord tissue, are scattered throughout the spinal cord and contribute to the recovery of oligodendrocyte and astrocyte numbers after injury (Horner et al., 2000; Barnabe-Heider et al., 2010). The potential to modulate the proliferation and differentiation of endogenous precursor cells represents an attractive therapeutic

*Correspondence to: V. Martínez-Cerdeño, Institute for Pediatric Regenerative Medicine, 2425 Stockton Boulevard, Sacramento, CA 95817, USA. Tel: +1-916-453-2163; fax: +1-916-453-2288.
E-mail address: vmartinezcerdeno@ucdavis.edu (V. Martínez-Cerdeño).
Abbreviations: BMS, Basso Mouse Scale; CC, central canal; DGM, dorsal gray matter; DWM, dorsal white matter; GFAP, glial fibrillary acidic protein; PBS, phosphate buffered saline; PFA, paraformaldehyde; SCI, spinal cord injury; VGM, ventral gray matter; VWM, ventral white matter.

0306-4522/13 $36.00
http://dx.doi.org/10.1016/j.neuroscience.2013.09.011

target for SCI. Although recent human clinical trials have demonstrated safe transplantation of stem cells into the human spinal cord (Karussis et al., 2010; Mazzini et al., 2010; Glass et al., 2012), the introduction of allogeneic stem cells still raises safety and ethical concerns. The capacity to modify endogenous precursor cell properties is thus a good alternative to stem cell transplantation.

Previous studies on progenitor cell properties after SCI have quantified levels of cell proliferation within specific areas of the spinal cord or the overall proliferation of specific progenitor cell types. In the current study, we investigated the level of proliferation and cell fate of newly generated cells within specific anatomical regions – dorsal and ventral portions of the white and gray matter – and specific segments – rostral and caudal to the injury site. Distinct cell populations, located within different regions of the spinal cord, fulfill specific functions. For example, the dorsal gray matter (DGM) is populated by sensory interneurons whereas the ventral gray matter (VGM) contains the motor neurons, and both regions contain glial cells (Watson et al., 2009). The white matter of the spinal cord consists primarily of oligodendrocytes and bundles of axons organized into distinct tracts with specific functions (Watson et al., 2009). Specific cell populations may be the result of distinct pools of precursor cells with distinct differentiation potentials, thus generating differential responses across anatomical regions of the spinal cord. Successful regenerative therapies will need to account for the anatomical organization of the spinal cord and the unique needs of each region for repair.

Prior work in this field has focused on transection or contusion models of SCI, whereas the proliferative response to the lateral compression injury model of SCI has not been previously characterized to the same extent. The compression model of SCI is widely used because of its ease of use, low cost, reproducibility, and pathological features which closely mimic clinical cases of SCI in humans (Plemel et al., 2008; Marques et al., 2009). We hypothesize that precursor cell proliferation after a moderate compressive SCI in mice follows a specific temporal and spatial pattern for proliferation and cell fate. By labeling cells undergoing mitosis in response to injury with BrdU, we tracked precursor cell proliferation levels, and using immunohistochemistry for specific cell markers we determined cell fate and population dynamics, throughout the first 14 days after injury. We observed that proliferation was greater at the injury epicenter than in adjacent rostral and caudal spinal segments. Additionally, we found that at early time-points after injury, $BrdU^+$ cells mainly expressed microglial/macrophage and astrocytic markers, while at these same time-points in the control spinal cord, the mitotic cells predominantly expressed markers for mature oligodendrocytes and oligodendrocyte precursors.

EXPERIMENTAL PROCEDURES

Spinal cord compression injury

We anesthetized female Swiss Webster adult mice (25–35 g, 6–8 weeks old; Charles River, Wilmington, MA) with isoflurane (4% to induce and 2% to maintain; Phoenix Pharmaceutical, Inc., Burlingame, CA, USA). After disinfection of the dorsal area between the neck and hind limbs, we made a midline incision to expose the spinal column at the level of T8–T11, and a laminectomy on the 10th thoracic vertebra. We laterally compressed the spinal cord to a thickness of 0.35 mm and held for 15 s using one pair of modified forceps (Plemel et al., 2008). After injury, we sutured the muscles and closed the skin. Post-operatively, we administered saline and prophylactic Baytril (85 mg/kg/day; Bayer) and maintained the animals on an isothermic pad until alert and mobile. The analgesic we administered was pharmaceutical grade bupronepherine (0.05 mg/kg), given every 12 h post-operatively. We expressed the animals' bladders manually twice daily until the animals were capable of self-voiding. We continually evaluated animals for weight loss, dehydration, discomfort, infection, and autophagia, with appropriate veterinary care administered as needed. The experimental study was designed following National Institutes of Health (NIH) guidelines and with the approval of the University of California, Davis Institutional Animal Care and Use Committee (IACUC).

Behavioral testing

Basso Mouse Scale (BMS). The BMS for locomotion was performed as previously described (Basso et al., 1996).

Rotarod. Animals were placed on a Rotamex with a starting speed of 0 rpm. The speed increased by intervals of 0.5 rpm every 5 s and the time that the animal fell off was recorded.

Von Frey hair test. To test for sensory function after injury, we performed the von Frey hair test as previously described (Chaplan et al., 1994). The minimal amount of force, in grams, that elicited a withdrawal response was recorded.

Ethyl chloride test. A spray of ethyl chloride was applied to animal's hind paws. A score of 1 indicated no response; a score of 2 indicated withdrawal and licking of the paw, and sometimes a vocalization; a score of 3 demonstrated a marked response with withdrawal, jumping, and multiple vocalizations. The trial was repeated three times on each paw, with a time period of 5 min between each trial to prevent desensitization to the stimulus.

5-Bromodeoxyuridine labeling

To determine cell proliferation and fate during the acute phase of injury, we injected mice immediately after surgery with 50 mg/kg of body weight BrdU (Sigma, St. Louis, MO, USA) intra-peritoneally and then administered follow-up injections of BrdU every 12 h until perfusion 1, 3, 5, 9, or 14 days after injury.

Immunocytochemistry

We administered Avertin (IP 0.2 ml/10 g of body weight; Sigma, St. Louis, MO, USA) to adult mice and perfused intracardially with room temperature phosphate-buffered saline (PBS) followed by ice-cold 4% paraformaldehyde (PFA). We removed the spinal cords, post-fixed them for 24 h in PFA, and then embedded segments in 3% agarose. After embedding, we cut 50-μm coronal slices on a vibratome (Leica, Wetzlar, Germany). To allow BrdU antibodies to bind to their target in the cell nuclei, we post-fixed free-floating tissue in 4% PFA for 15 min, washed in PBS, and then incubated at 37 °C in 2 N HCl for 30 min. We then blocked sections in 10% donkey serum (Gibco, Grand Island, NY, USA) and 0.1% Triton X-100 (Sigma, St. Louis, MO, USA) and incubated tissue for 24 h at room temperature in primary antibodies which include: rat anti-BrdU conjugated to FITC or TexasRed (Abcam, Cambridge, MA, USA, 1:200), goat anti-Olig2 (R&D Systems, Minneapolis, MN, USA, 1:1000), chicken anti-neuronal specific nuclear protein (anti-MAP2; Millipore, Billerica, MA, USA, 1:1000), mouse anti-GFAP (Sigma, St. Louis, MO, USA, 1:400), mouse anti-Nestin (Chemicon, Billerica, MA, USA, 1:50), mouse anti-neuronal nuclei (anti-NeuN; Millipore, Billerica, MA, USA, 1:1000), rabbit anti-Iba1 (Wako, Richmond, VA, USA, 1:500), and rabbit anti-S100b (Abcam, Cambridge, MA, USA, 1:500). Following incubation in the primary antibodies, we rinsed sections in PBS and incubated them for 1 h with appropriate secondary antibodies: Dylight-488, Dylight-555, or DyLight-649 conjugated polyclonal donkey anti-mouse/goat/rabbit/chicken antibodies (Jackson Lab., West Grove, PA, USA, 1:100). We diluted all antibodies in incubation buffer containing 1% donkey serum (Gibco, Grand Island, NY, USA) and 0.01% Triton X-100 (Sigma, St. Louis, MO, USA). As a control, we omitted the first antibody for each experiment. We used the nuclear marker DAPI (Molecular Probes, Grand Island, NY, USA, 1:1000) for cytoarchitectural reference.

Nissl staining

Tissue was mounted on slides and incubated overnight in a 1:1 solution of 100% ethanol and chloroform. Slides were then put in a solution of 100% ethanol for 1 min, transferred to 95% ethanol for 1 min, transferred to 70% ethanol for 1 min, and then put in de-ionized water for 1 min. Slides were then transferred to a Crystal Violet solution for 5–10 min to achieve optimal staining. After Crystal Violet incubation, slides were dipped in de-ionized water, then 70% ethanol, and incubated in 100% ethanol for 2 min. The tissue was checked to ensure it did not need further staining with Crystal Violet, then washed twice in 100% ethanol for 5 min and washed twice in xylene for 5 min.

Cell quantification

We performed all imaging on a Nikon C-1 confocal microscope using Nikon EZC1 3.0 software (Nikon, Melville, NY, USA). After imaging, we exported data to Adobe Photoshop CS4 (Adobe, San Jose, CA, USA) for quantification of cells. We quantified on the basis of the BrdU immunostaining colocalizing with DAPI. Once we counted $BrdU^+$ cells, we assessed their colocalization with other markers. We characterized cells as either dorsal or ventral using the middle of the central canal (CC) as a determining landmark. Furthermore, we characterized cells as located within the gray or white matter (Fig. 1A). We counted $BrdU^+$ cells in the CC as a separate category, and only cells that were clearly contacting the CC were included in this group. Upon removal of the spinal cord and prior to sectioning, we cut 2-mm blocks of the spinal cord: the epicenter, which comprised of ± 1 mm of the compression; rostral, which consisted of the spinal cord 1–3 mm rostral of the injury site; and caudal, which was the segment of the spinal cord 1–3 mm caudal of the injury location (Fig. 1B). We quantified three 50-μm slices from each region (rostral, epicenter, caudal) for each data set. Three mice were used for each time point and we pooled results for analysis.

Statistical analysis

We analyzed data with Microsoft Excel 12.1 and GraphPad Prism 5. We expressed values as means ± SEM. We assessed significance of the differences between means by one-way analysis of variance (ANOVA) followed by the Bonferroni test. A probability of less than 5% ($P < 0.05$) was considered to be statistically significant.

RESULTS

The lateral compression SCI model

The calibrated forceps compression model of SCI was created by Plemel et al. (2008) and has been validated and utilized by others (Marques et al., 2009). We compressed the mouse spinal cord to a diameter of 0.35 mm. We found that doing so generated a reproducible injury, as assessed by histological and behavioral studies (Fig. 1). Histology demonstrates marked cytoarchitectonic disruptions, yet the boundary between the white and gray matter could still be distinguished even in the injury epicenter (Fig. 1A, B). We performed motor and sensory behavioral testing prior to surgery and again 1–4, 6, 8, 10, and 12 weeks after injury or laminectomy. After injury, animals demonstrated impaired motor and sensory function compared to control animals, which received a laminectomy only. On the BMS for locomotor function, injured animals reached an average score of 4.5 ± 0.7 after three weeks, and their performance score remained constant at later time points, compared with a score of 9 for animals which received a laminectomy only, indicating this latter group was unaffected by the procedure (Fig. 1C). Furthermore, when tested on the rotarod, injured animals consistently fell off at earlier times than laminectomy-only animals (Fig. 1D; p-value < 0.05). Prior to injury, the average duration a mouse could stay on the rod was 194 ± 19 s. One

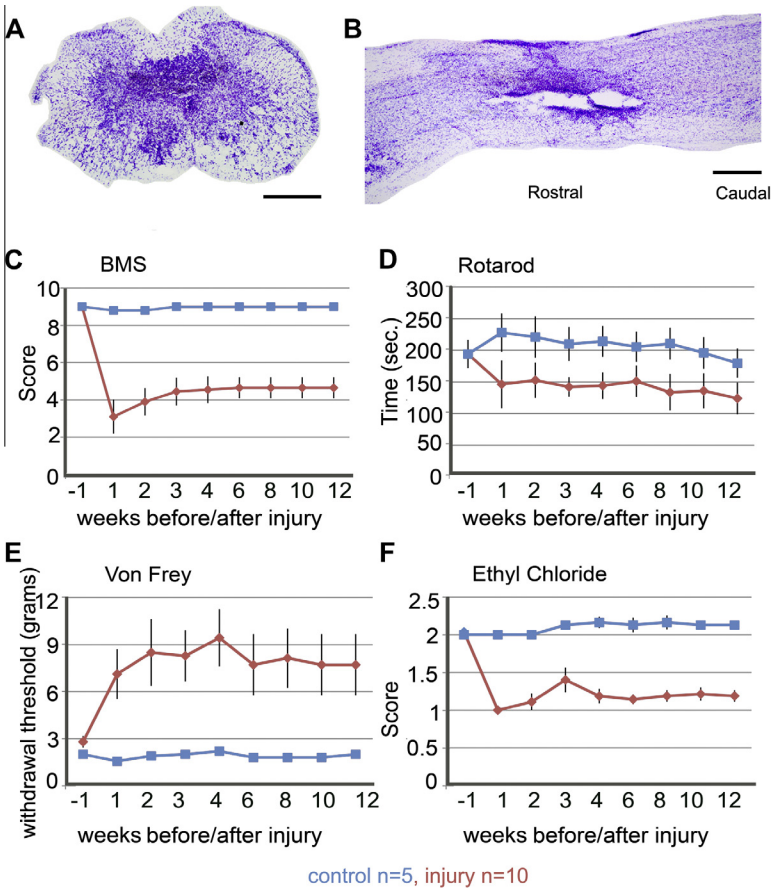

Fig. 1. Characterization of the lateral compression injury model. (A) Transverse section of Nissl-stained spinal cord 7 days after injury. (B) Sagittal section of Nissl stained spinal cord 7 days after injury. (C–F) Behavioral testing data over a twelve week period, with control animals indicated in blue and injured animals indicated in red. (C) Basso Mouse Scale score in animals after compressive spinal cord injury or laminectomy. (D) Performance on the rotamex after injury or laminectomy. (E) Von Frey hair test to assess sensitivity after laminectomy or injury. (F) Ethyl chloride test to detect sensory function after injury or laminectomy. (For interpretation of the references to color in this figure legend, the reader is referred to the web version of this article.)

week after surgery, those that had received a compression injury had an average duration of 146 ± 14 s compared to laminectomy-only animals that had an average duration of 228 ± 29 s. After 2 weeks, injured animals could stay on the rod for an average of 152 ± 15 s compared to laminectomy-only animals that could stay on the rod an average of 221 ± 21 s. At the 3 and 4 week time-points, injured animals had averages of 142 ± 26 s and 143 ± 24 s, respectively. At these same time-points, control animals averaged 209 ± 15 s and 214 ± 21 s. At a later time-point of 10 weeks, injured animals averaged a duration of 133 ± 25 s compared to 196 ± 27 s for controls. Injured animals also had impaired sensory function as measured by the von Frey hair test (Fig. 1E; p-value < 0.05), in which a greater force had to be applied to their hind paws to elicit a withdrawal response than the control group. Control animals at all time points responded to a force of approximately 1.8 ± 0.2 g, whereas injured animals responded to an average force of 8.0 ± 1.8 g. Similarly, injured animals demonstrated reduced sensitivity to the application of ethyl chloride to their hind paws (Fig. 1F; p-value < 0.05). Control animals responded to the application of ethyl chloride by withdrawing and licking affected paws (score of 2), whereas injured animals generally demonstrated a non-response (score of 1). Overall our behavioral data indicates that a plateau of locomotor and sensory function is reached after three weeks and the injury is consistent among multiple animals.

Proliferation in the intact spinal cord

We first examined proliferation in the intact spinal cord. We performed a laminectomy at the level of the tenth thoracic vertebra (T10) and administered BrdU immediately after surgery. To identify newly generated cells during the acute injury phase and follow them throughout the study, we administered intraperitoneal BrdU the day of the injury and each day thereafter until the animals were sacrificed for analysis. We sacrificed animals 1, 3, 5, 9, and 14 days after SCI. To quantify the rate of proliferation, we cut 50-μm traverse sections of spinal cord spanning from 3-mm rostral to 3-mm caudal of the injury epicenter. We classified these sections as specific rostro-caudal segments; we consider sections within ± 1 mm from the center of the injury as epicenter, sections within 1–3 mm caudal of the injury as caudal, and sections within 1–3 mm rostral of the lesion center as rostral (Fig. 2B). We

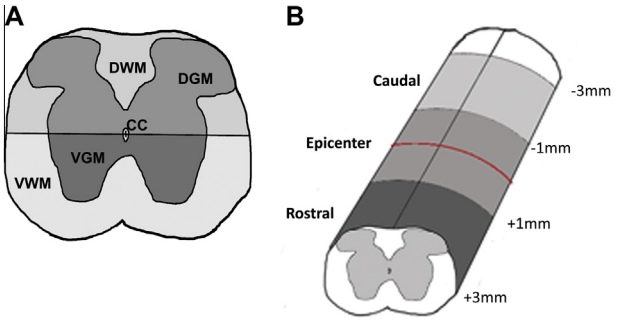

Fig. 2. Scheme depicting the spinal cord regions used for BrdU$^+$ cell number quantification. (A). BrdU$^+$ cells were quantified based on localization in the dorsal or ventral region of the spinal cord using the midline of the central canal as the boundary landmark. Cells were further classified by localization within the white or gray matter. We quantified cells within five distinct anatomical regions: dorsal gray matter (DGM), dorsal white matter (DWM), ventral gray matter (VGM), ventral white matter (VWM), and central canal (CC). (B) We classified the injury epicenter as the tissue spanning ± 1 mm from the center of the lesion. Rostral sections of tissue were 1–3 mm rostral from the center of the lesion, and caudal sections were 1–3 mm caudal from the center of the lesion.

characterized cells within each of the slices as either dorsal or ventral using the CC as the boundary landmark. Furthermore, we characterized cells based on location in the gray or white matter (Fig. 2A). We classified CC cells as BrdU$^+$ cells with a soma that was clearly contacting the CC. We quantified the number of BrdU$^+$ cells in three slices of spinal cord from each segment and averaged the total number of each cell type within each segment/region.

The rate of proliferation was low in the parenchyma of laminectomy-only (control) spinal cords. After 1 day of BrdU labeling, we quantified an average of 6.0 ± 0.50 cells in a 50-μm-thick spinal cord transversal section. The average number of BrdU$^+$ cells was 18.8 ± 1.0 cells per section on day three, 72.7 ± 6.7 cells on day 5, 205 ± 8.9 cells on day 9, and 414 ± 12.7 on day 14. The increase in the average number of cells per section in the control spinal cord was approximately linear through time (Fig. 3A). Across the three rostro-caudal segments – rostral, epicenter, and caudal – the rate of proliferation was similar at all time-points (Fig. 3C; *p*-values > 0.05). Distribution of BrdU$^+$ cells within the intact spinal cord across anatomical regions was not homogeneous; the VGM of the control spinal cord consistently had fewer BrdU$^+$ cells than other regions of the spinal cord at all time-points except at 14 days (Fig. 3D; *p*-values < 0.05). Cumulative proliferation in the CC of uninjured spinal cord tissue was low, ranging from an average of 0.13 ± 0.04 to 0.55 ± 0.09 cells during the first 5 days. This number increased to 2.0 ± 0.22 cells at day 9 and was similar after 14 days of BrdU administration (Fig. 3B).

Proliferation in the parenchyma of the injured spinal cord

The increase in the number of BrdU$^+$ cells was greater in injured than in the control spinal cord. One day after injury, there was an average of 48.7 ± 4.0 cells per 50-μm section, an increase of 8.2-fold compared to the control spinal cord at the same time-point. Three days after injury, the number of BrdU$^+$ cells increased 11.8-fold from the previous time-point to an average of 577 ± 37 cells per 50-μm section. The rate of proliferation slowed by 5 days, when there was an average of 938 ± 68 cells per 50-μm section, an increase of 1.6-fold from the 3-day time-point. The rate of increase in BrdU$^+$ cells showed a slowing trend between 9 and 14 days, where we quantified averages of 1234 ± 58.0 and 1430 ± 60.8 BrdU$^+$ cells, respectively. The apparent rate of increase in the number of BrdU$^+$ cells between 9 and 14 days was similar between control and injured spinal cord (Fig. 3A). We found the greatest number of BrdU$^+$ cells at the injury epicenter during early time-points; at later time-points the number of BrdU$^+$ cells in the caudal sections increased and became comparable to values found in the epicenter (*p*-values > 0.05) and significantly increased compared to rostral areas (Fig. 3C′; *p*-values < 0.05).

The distribution of BrdU$^+$ cells across anatomical regions after injury varied over time, following a pattern different from the control spinal cord. One day after injury, the number of BrdU$^+$ cells in the VGM, DGM, and dorsal white matter (DWM) were comparable (*p*-values > 0.05), but differed significantly from the ventral white matter (VWM) (*p*-value < 0.0001). At days 3, 5, and 9, the VGM had significantly fewer cells than the VWM and DGM (*p*-values < 0.05), but was comparable to the DWM (*p*-values > 0.05). 14 days after injury the trend of fewer BrdU$^+$ cells in the VGM was restored, although there was still a significant difference between the dorsal white and gray matter that was not observed in control tissue (*p*-value < 0.05).

Proliferation in the CC of the injured spinal cord

One day after injury, there was an average of 0.25 ± 0.05 BrdU$^+$ cells at the CC. Statistical analysis indicated that this small increase was significant compared with the control spinal cord (*p*-value = 0.02). After injury, the number of BrdU$^+$ cells at the CC continued to increase (Fig. 3B). Three days after injury, the number of BrdU$^+$ cells increased 10-fold to 2.5 ± 0.27 cells, and 5 days after injury the number increased 1.4-fold compared to the previous time-point, reaching an average of 3.4 ± 0.37 cells. Between 5 and 9 days, there was an increase of 1.7-fold, and between 9 and 14 days an increase of 1.3-fold. Thus, cell proliferation of the CC followed a similar time-course as that of parenchymal proliferation, with the greatest increase occurring between 1 and 3 days after injury. However, unlike the parenchymal proliferation, which showed a leveling off or return to control rates of proliferation between 9 and 14 days, proliferation at the CC was still occurring at an increased rate compared with the control spinal cord.

Cell fate of newly generated BrdU$^+$ cells

We performed double and triple immuno-labeling to determine BrdU$^+$ cell marker expression at each

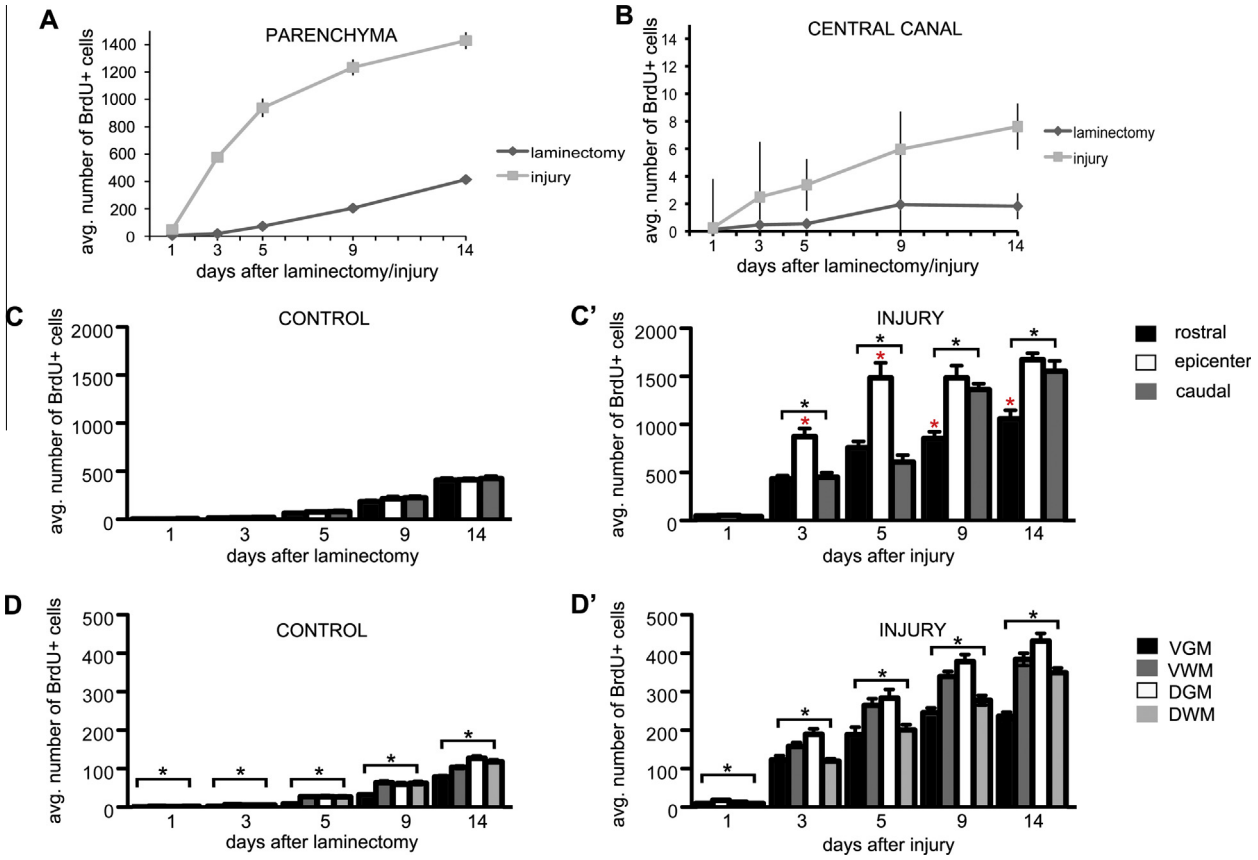

Fig. 3. Average number of BrdU$^+$ cells per 50-μm-thick slice categorized by injury proximity and spinal cord region. (A) Average number of BrdU$^+$ cells over time in the spinal cord parenchyma. The average number of BrdU$^+$ cells increased linearly in control tissue, whereas there was an initially exponential increase in the number of positive cells in injured tissue. (B) Average number of BrdU$^+$ cells over time in the central canal of the spinal cord. The average number increased very slowly in control tissue and rapidly after injury. (C) Average number of BrdU$^+$ cells by proximity to the laminectomy site. The average number was homogeneous across segments (p-values > 0.05). (C′) Average number of BrdU$^+$ cells by proximity to the injury site. During early time points the average number of cells increased in the epicenter, followed by an increase in cell proliferation caudal of the injury site. Bars and black * indicate significance in ANOVA, whereas red * indicates significance in post hoc tests. (D) Average number of BrdU$^+$ cells by anatomical region in the control tissue. At nearly all time points, there were fewer BrdU$^+$ cells in the ventral gray matter (VGM) (p-values < 0.05). (D′) Average number of BrdU$^+$ cells by anatomical region in injured tissue. The numbers of BrdU$^+$ cells were lower in the ventral gray matter and the dorsal white matter of injured than in the control spinal cord. Bars and black * indicate significance in ANOVA. (For interpretation of the references to color in this figure legend, the reader is referred to the web version of this article.)

time-point. We found that BrdU$^+$ cells expressed a variety of markers for precursor cells, such as Nestin (Fig. 4A) and Olig2 (Fig. 4B), oligodendrocytes (Sox10; Fig. 4C), mature astrocytes (glial fibrillary acidic protein (GFAP) and S100b; Fig. 4D, E), microglia (Iba1; Fig. 4F), and for mature and immature neurons (MAP2 and NeuN, respectively). No BrdU$^+$ cells at any time-point in the control spinal cord (17,075 BrdU$^+$ cells) or in the injured spinal cord (115,024 BrdU$^+$ cells) expressed MAP2 and/or NeuN, indicating that none of the newly generated cells acquired neuronal fates.

The number of BrdU$^+$ cells that expressed specific markers differed among segments and regions of the spinal cord, but there was a significant increase in both the total number of BrdU$^+$ cells after injury, as well as the total number of BrdU$^+$ cells that were also positive for specific markers. We reasoned that comparing the total numbers of cells would not sufficiently describe cell fate dynamics of specific cell populations after injury. Additionally, differences in total cell numbers between segments and regions would be influenced by variations in the area of each segment and region of interest. To elucidate meaningful cell fate dynamics after injury, we therefore analyzed the percentage of BrdU$^+$ cells that also expressed a specific marker within each segment and region of the spinal cord. Although total cell numbers increased with time, for some cell populations the proportion of BrdU$^+$ cells expressing a specific marker was unaltered by injury, while for other cell populations this proportion changed markedly over time. Focusing on the proportion of double-positive cells compared to the total number of BrdU$^+$ cells at each time point in the various segments and regions of the intact and injured spinal cord allowed us to evaluate changes in cell populations over time and draw conclusions about the progenitor cell response to SCI.

Co-expression of the progenitor marker Nestin with BrdU varied significantly between control and injured spinal cord at early time points, but at intermediate times (5 and 9 days), the percentage of double-positive cells between the two conditions approached similar values (Fig. 5A). In the control spinal cord,

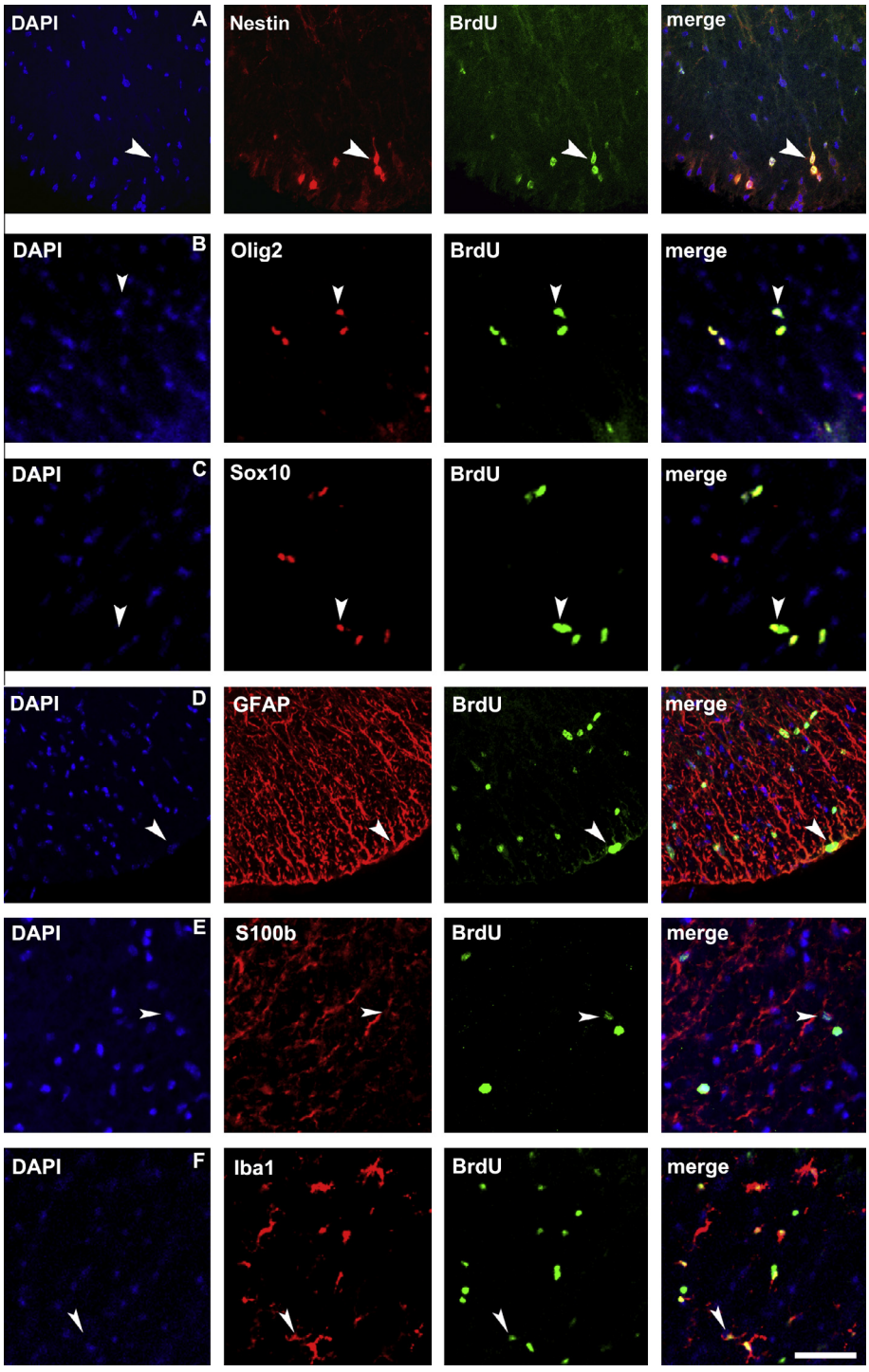

Fig. 4. Representative images of BrdU$^+$ cells within the injured spinal cord 3 days after injury. All images were taken from a rostral section of the spinal cord in the ventral white matter 3 days after injury. BrdU$^+$ cells (red) colocalized with a variety of markers (green) for progenitor cells (Nestin – (A) and Olig2 – (B)), oligodendrocytes (Sox10 – C), astrocytes (GFAP – (D) and S100B – (E)), and microglia (Iba1 – (F)). Arrows point out a single representative BrdU$^+$ cell expressing the marker of interest, although other examples are present in the images. Scale bar = 100 μm. (For interpretation of the references to color in this figure legend, the reader is referred to the web version of this article.)

BrdU$^+$/Nestin$^+$ cells were not present until after 5 days of continuous BrdU administration. However, 1 day after injury, 15.7 ± 1.7% of BrdU$^+$ cells were Nestin$^+$. The proportion of double-positive cells after injury fluctuated little through time. The proportion varied between 5.35 ± 0.41% and 17.02 ± 0.99% during the experiment. In the control spinal cord, the distribution of BrdU$^+$/Nestin$^+$ cells was homogeneous between rostral, epicenter, and caudal segments (*p*-values > 0.05; Fig. 5B). After injury, there was a large increase in the proportion of BrdU$^+$/Nestin$^+$ cells at the injury epicenter (Fig. 5B′), where 21.4 ± 3.0% of BrdU$^+$

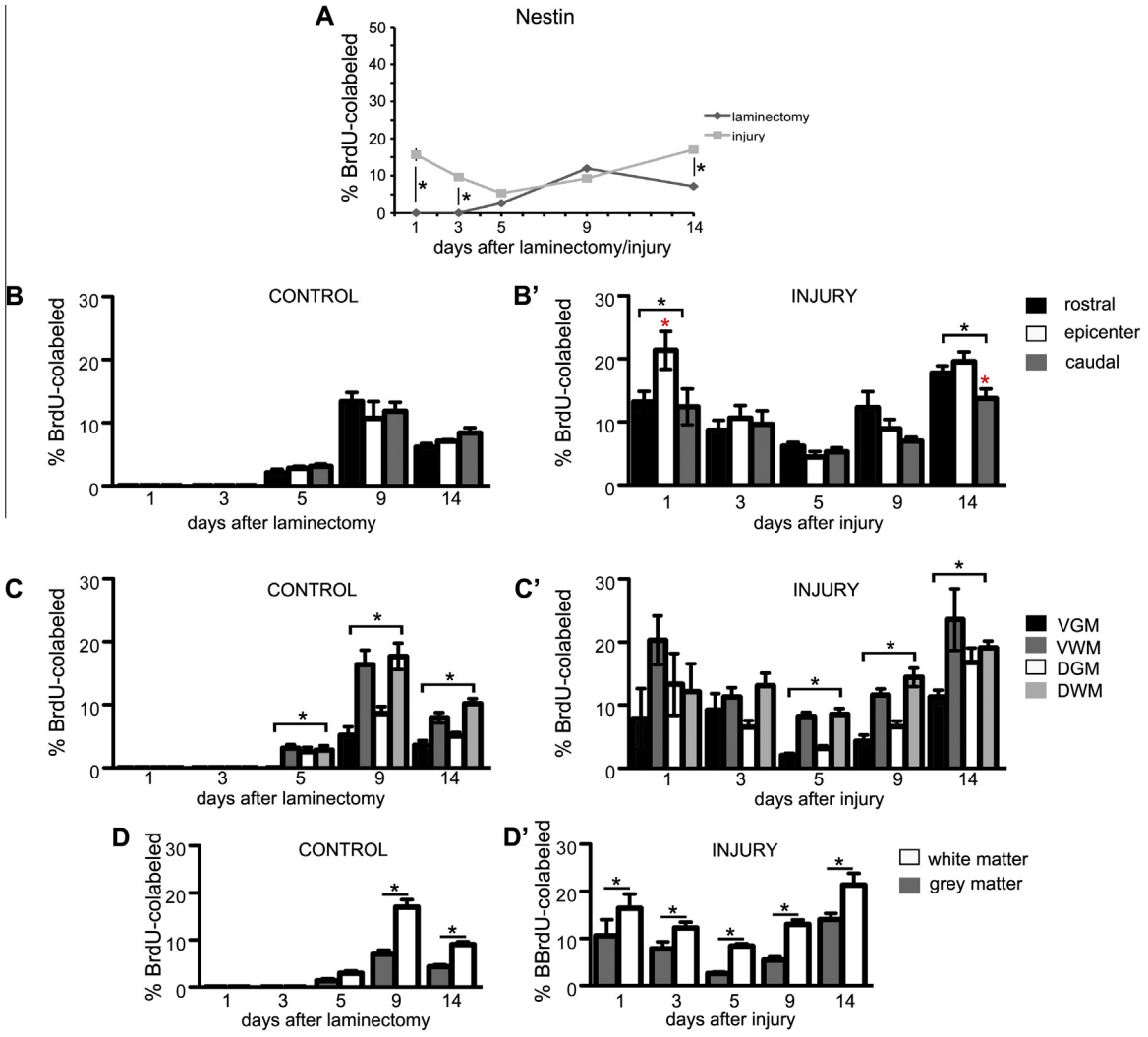

Fig. 5. Proportion of BrdU$^+$ cells colabeling with Nestin in control and injured spinal cord. (A) No BrdU$^+$/Nestin$^+$ cells were present in control tissue before 5 days, but within 1 day after injury there were double-positive cells present. The proportion of BrdU$^+$/Nestin$^+$ cells after injury showed a downward trend toward 5 days, followed by a later upward trend. (B) Proportion of BrdU$^+$/Nestin$^+$ cells was homogeneous with respect to the location of the laminectomy (p-values > 0.05). (B′) The proportion of double-positive cells increased at the epicenter 1 day after injury, then levels decreased across all regions. Bars and black * indicate significance in ANOVA, whereas red * indicates significance in post hoc tests. (C) Control tissue had a higher proportion of double-positive cells in the ventral and dorsal white matter. (C′) The proportion of double-positive cells in different anatomical regions varied greatly after injury, though showed a similar trend of increasing in the ventral and dorsal white matter. Bars and black * indicate significance in ANOVA. (D, D′) Overall the proportion of BrdU$^+$/Nestin$^+$ cells was greater in the white matter than the gray matter of the spinal cord (p-values < 0.05). (For interpretation of the references to color in this figure legend, the reader is referred to the web version of this article.)

cells co-expressed Nestin compared to 13.2 ± 1.7% and 12.4 ± 2.9% in adjacent segments. At later time-points, the difference in proportion of BrdU$^+$/Nestin$^+$ cells between rostro-caudal segments in the injured spinal cord decreased and was non-significant. In the control spinal cord, a higher percentage of double-positive cells were present in the ventral and DWM (Fig. 5C), a trend that was re-established after 5 days in the injured spinal cord (Fig. 5C′). Overall, a greater percentage of BrdU$^+$/Nestin$^+$ cells were present in the white matter than in the gray matter, both in intact and injured spinal cord (Fig. 5D, D′).

The predominant marker co-expressed by BrdU$^+$ cells in the control spinal cord was Olig2, a marker for oligodendrocyte precursor cells, which may also be transiently expressed by astrocytes (Chen et al., 2012). Expression of this marker was drastically reduced after injury (Fig. 6A). After 1 day of BrdU labeling, the proportion of BrdU$^+$/Olig2$^+$ cells was 90.8 ± 3.8% per slice in the control spinal cord, whereas 1 day after injury the proportion was 41.5 ± 4.59%. This proportion decreased over time to a low of 19.4 ± 1.05% at 9 days after injury, and displayed an upward trend at 14 days. In the control spinal cord, the proportion of BrdU$^+$/Olig2$^+$ cells also decreased significantly between 5 and 9 days.

The proportion of BrdU$^+$ cells expressing Olig2 across segments and regions was homogeneous in the control spinal cord (rostro-caudal: p-values > 0.05; dorso-ventral: p-values > 0.05; gray-white matter:

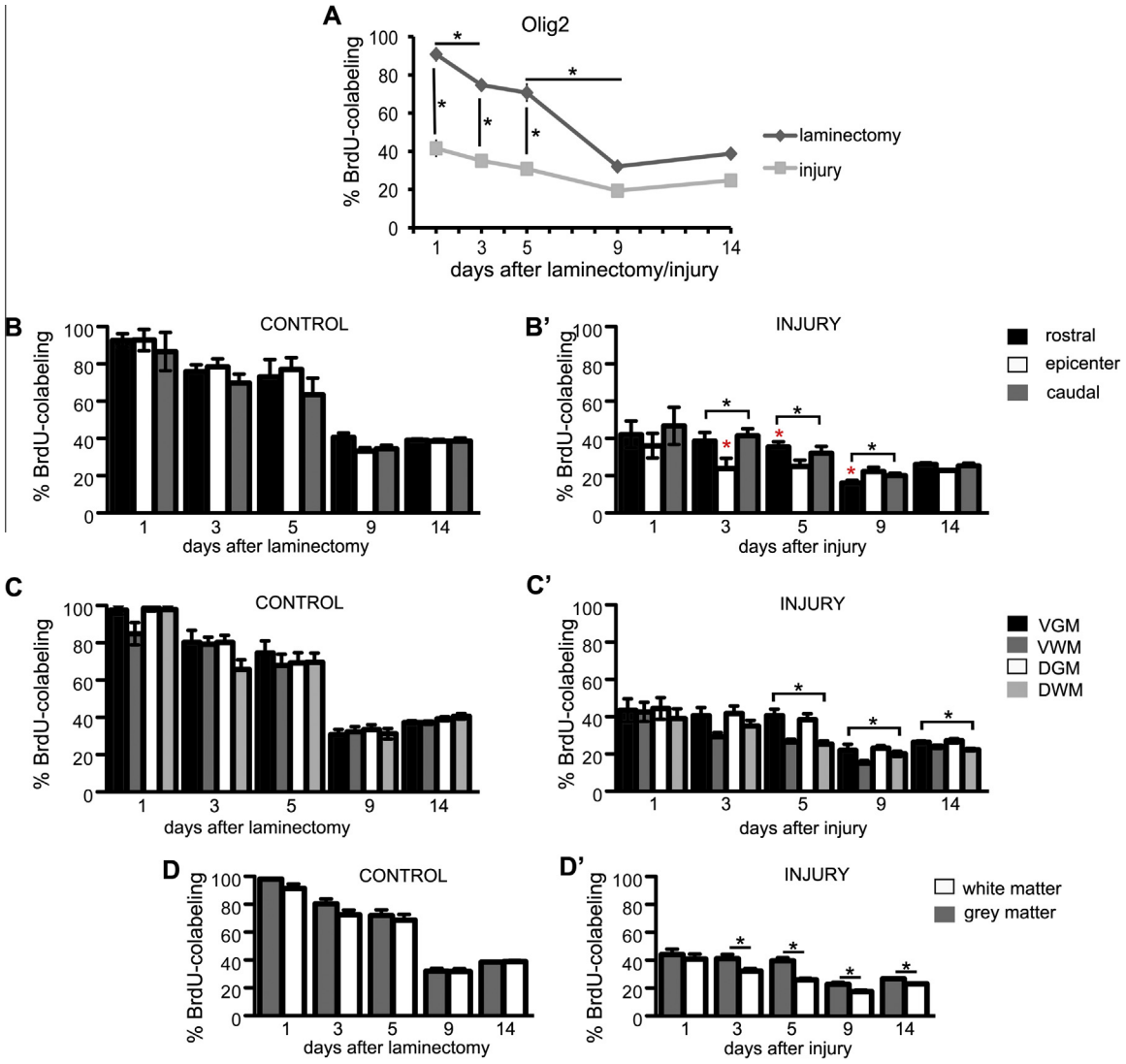

Fig. 6. Proportion of BrdU$^+$ cells colabeling with Olig2 in control and injured spinal cord. (A) Proportion of double-positive cells at all time points and conditions. The percentage of double-positive cells decreased over time for both groups, but was drastically lower 1–5 days after injury. The proportion of cells returned to nearly control levels after 9 days. (B) The proportion of BrdU$^+$/Olig2$^+$ cells was homogeneous with respect to the location of the laminectomy (p-values > 0.05). (B′) However, the proportion of double-positive cells decreased at the injury epicenter 3 days after laminectomy. Bars and black * indicate significance in ANOVA, whereas red * indicates significance in post hoc tests. (C) There was no variation within anatomical regions in control tissue (p-values > 0.05). (C′) The proportion of double-positive cells decreased in the ventral white matter after 3 days and remained low through 9 days after injury. Bars and black * indicate significance in ANOVA. (D) The proportion of double-positive cells in the white and gray matter was equal after laminectomy (p-values > 0.05) (D′) After injury, there were more BrdU$^+$/Olig2$^+$ cells in the gray matter than the white matter (p-values < 0.05). (For interpretation of the references to color in this figure legend, the reader is referred to the web version of this article.)

p-values > 0.05; Fig. 6B–D). However, it varied 3 days after injury (Fig. 6B′), when there was a lower proportion in the epicenter (24.0 ± 5.4%) relative to the rostral and caudal segments (38.7 ± 4.6% and 41.5 ± 3.8%, respectively). At later time-points, there was a continuous difference in the proportion of BrdU$^+$/Olig2$^+$ cells in the rostral spinal cord compared with other segments (p-values < 0.05; Fig. 6B′). The proportion of BrdU$^+$/Olig2$^+$ cells decreased noticeably in the VWM 3 days after injury (26.0 ± 1.5%) relative to the other regions, a change that was sustained through 9 days (Fig. 6C′). There was an increase in the proportion of BrdU$^+$/Olig2$^+$ cells in the gray matter from 3 days after injury until the end of the time-course, which did not occur in the control spinal cord (Fig. 6D, D′).

The proportion of BrdU$^+$ cells expressing Sox10, a marker of cells committed to the oligodendrocyte lineage, followed a similar time-course as BrdU$^+$/Olig2$^+$ cells. There was an initial decrease after injury in the proportion of Sox10-expressing BrdU$^+$ cells that ranged from 79.2 ± 3.6% to 51.6 ± 3.7%. However, it took 14 days for the proportion of Sox10$^+$ cells (Fig. 7A), and only 9 days for the proportion of BrdU$^+$/Olig2$^+$ cells, to recover to near control levels (Fig. 6A). The proportion of Sox10$^+$ cells was equal across the rostro-caudal segments and dorso-ventral regions of the

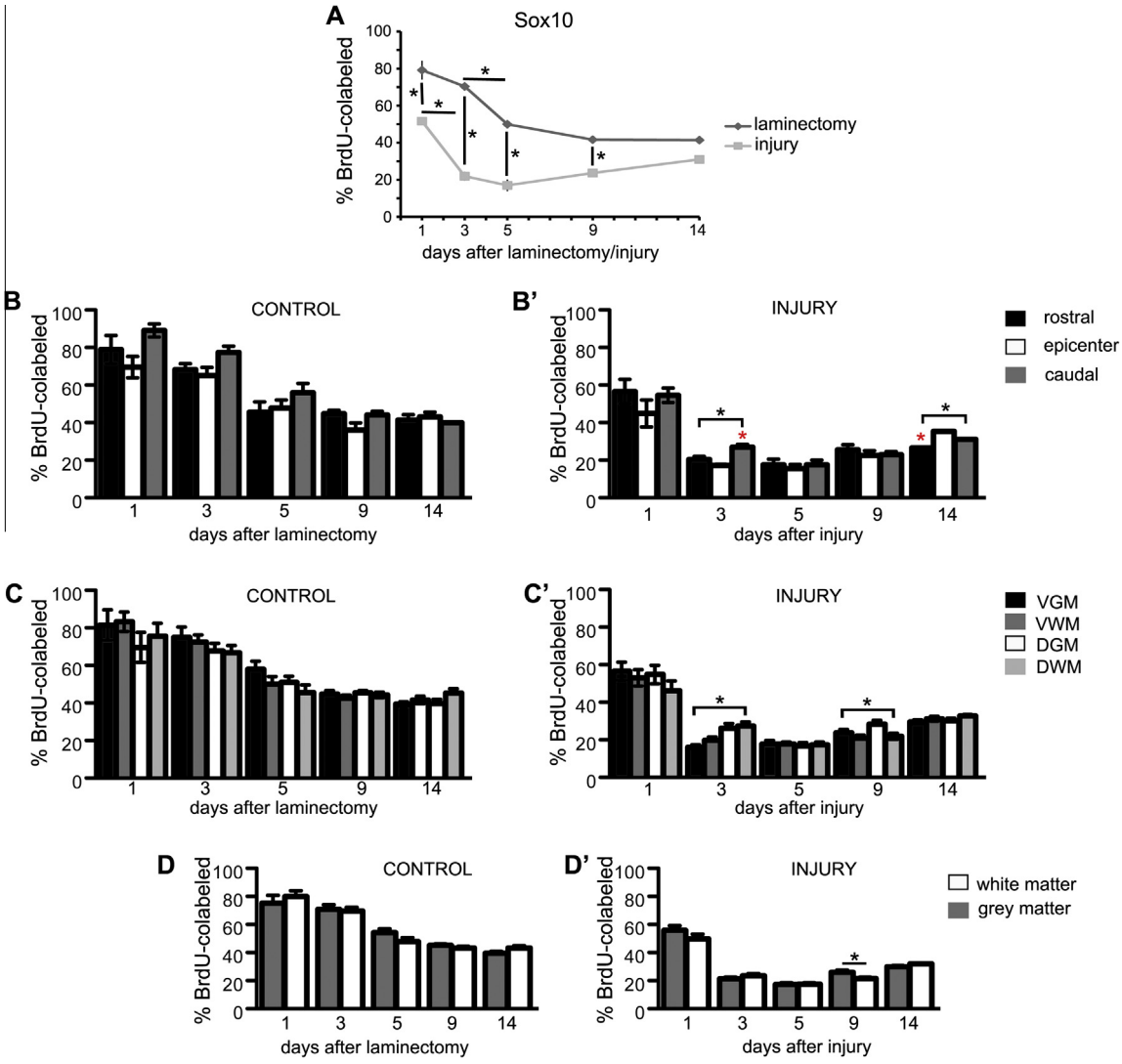

Fig. 7. Proportion of BrdU$^+$ cells colabeling with Sox10 in control and injured spinal cord. (A) Proportion of double-positive cells at all time points and conditions. The percentage of BrdU$^+$/Sox10$^+$ decreased over time for both groups, but was drastically lower 1 day after injury. The proportion of cells returned to nearly control levels after 14 days. (B) Proportion of BrdU$^+$/Sox10$^+$ cells was homogeneous with respect to the location of the laminectomy (p-values > 0.05). (B′) The proportion of double-positive cells decreased in most spinal cord regions after injury, but was slightly elevated in the caudal spinal cord 3 days after injury and slightly decreased in the rostral spinal cord after 14 days. Bars and black * indicate significance in ANOVA, whereas red * indicates significance in post hoc tests. (C) There was no variation when proportions were compared across anatomical regions in the control tissue (p-values > 0.05). (C′) However, the proportion of double-positive cells decreased in the ventral spinal cord after 3 days. Bars and black * indicate significance in ANOVA. (D)There was little variation in proportions of BrdU$^+$/Sox10$^+$ cells between white and gray matter in the control spinal cord. (D′) After injury there were approximately equal proportions of Sox10$^+$ cells in the white and gray matter except for a transient increase in the gray matter after 9 days. (For interpretation of the references to color in this figure legend, the reader is referred to the web version of this article.)

control spinal cord (Fig. 7C) (p-values > 0.05). After injury, there was variation in the distribution of BrdU$^+$/Sox10$^+$ cells within the rostro-caudal axis. Three days post-injury, there was a higher percentage of double-positive cells in the caudal spinal cord (27 ± 1.6%) compared with other segments (rostral = 20 ± 1.6 and epicenter = 17 ± 0.55%), and all three segments had varying proportions of BrdU$^+$/Sox10$^+$ cells at 14 days (Fig. 7B′). Three days after injury, there were more cells in the dorsal than the ventral spinal cord (Fig. 7C′), but otherwise BrdU$^+$/Sox10$^+$ cells were evenly distributed through the spinal cord after injury. These data showed less anatomical and temporal variability in the population of BrdU$^+$/Sox10$^+$ cells than was observed in BrdU$^+$/Olig2$^+$ cells after injury. However, there were similarities between the two populations, such as little variation observed between the distribution of BrdU$^+$/Olig2$^+$ cells between the gray and white matter regions after injury (p-values > 0.05, Fig. 6D, D′).

Of particular interest was the astrocyte response, which is a component of the inflammatory response initiated after injury. To assess the generation of new astrocytes after injury, we performed immunostaining with two separate markers for astrocytes, GFAP and

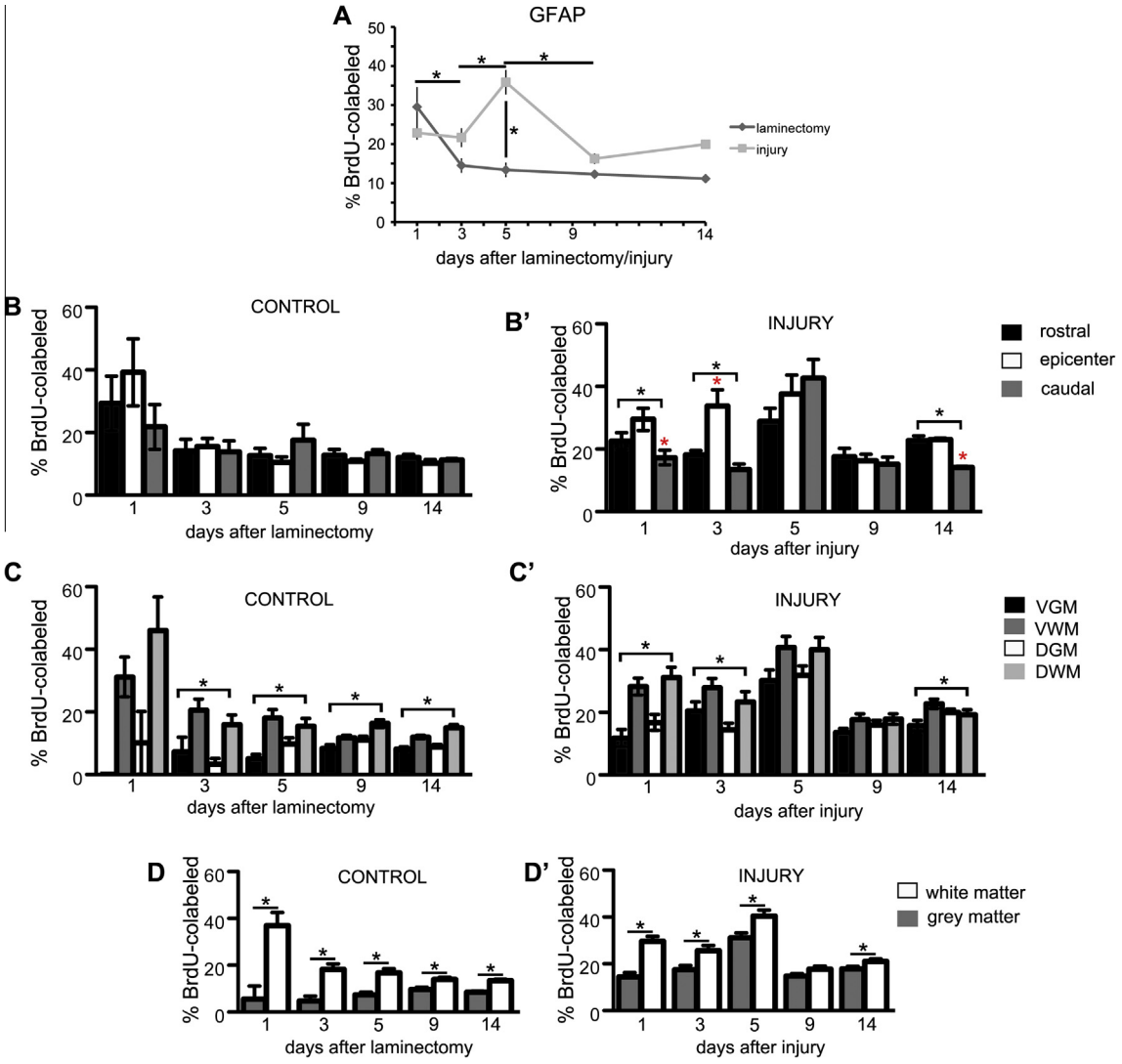

Fig. 8. Proportion of BrdU$^+$ cells colabeling with GFAP in control and injured spinal cord. (A) The percentage of double-labeled cells peaked 5 days after injury. (B) The proportion of BrdU$^+$/GFAP$^+$ cells was homogeneous with respect to the location of the laminectomy at time points after 3 days of continuous BrdU administration (p-values > 0.05). (B′) The proportion of double-positive cells increased at the epicenter relative to the caudal spinal cord 1 day after injury, then increased drastically at the epicenter after 3 days (p-values < 0.05). Bars and black * indicate significance in ANOVA, whereas red * indicates significance in post hoc tests. (C) Control tissue had a higher proportion of BrdU$^+$/GFAP$^+$ cells in the ventral and dorsal white matter than other regions. (C′) This trend was maintained after injury. Bars and black * indicate significance in ANOVA. (D, D′) Overall the proportion of BrdU$^+$/GFAP$^+$ cells was greater in the white matter than the gray matter of the spinal cord under both conditions. (For interpretation of the references to color in this figure legend, the reader is referred to the web version of this article.)

S100b. There was a transient increase in the proportion of BrdU$^+$ cells expressing GFAP that peaked 5 days after injury at 35.9 ± 3.2%, and decreased to near control levels 9 days after injury (Fig. 8A). There was a fair amount of variation in the control spinal cord after 1 day of BrdU administration with regard to the rostro-caudal axis and anatomical region of interest (Fig. 8B, C). In the control spinal cord, there were more BrdU$^+$/GFAP$^+$ cells in the white matter than in the gray matter (p-values < 0.05; Fig. 8D). This trend remained constant after injury (Fig. 8D′), however the difference between the white and gray matter narrowed and was non-significant 9 days after injury (p-value > 0.05). One day after injury, the proportion of BrdU$^+$/GFAP$^+$ cells was greater in epicenter segments (29.5 ± 3.5%) relative to caudal segments (17.3 ± 2.3%). After 3 days, there was a more pronounced increase in the number of BrdU$^+$/GFAP$^+$ cells at the epicenter (Fig. 8B′). As overall GFAP levels decreased after 5 days, expression of GFAP decreased in all segments. Once again, the proportion of BrdU$^+$/GFAP$^+$ cells increased slightly at 14 days in all segments except in the caudal spinal cord (p-values < 0.05). The distribution of double-positive cells after injury across dorso-ventral regions was similar to that in intact spinal cord (Fig. 8C′).

The proportion of BrdU$^+$/S100b$^+$ cells remained relatively unchanged between control and injured spinal cord (Fig. 9A). One day after injury, the percentage of BrdU$^+$/S100b$^+$ cells did not differ significantly between control and injured spinal cord (p-value > 0.05). A

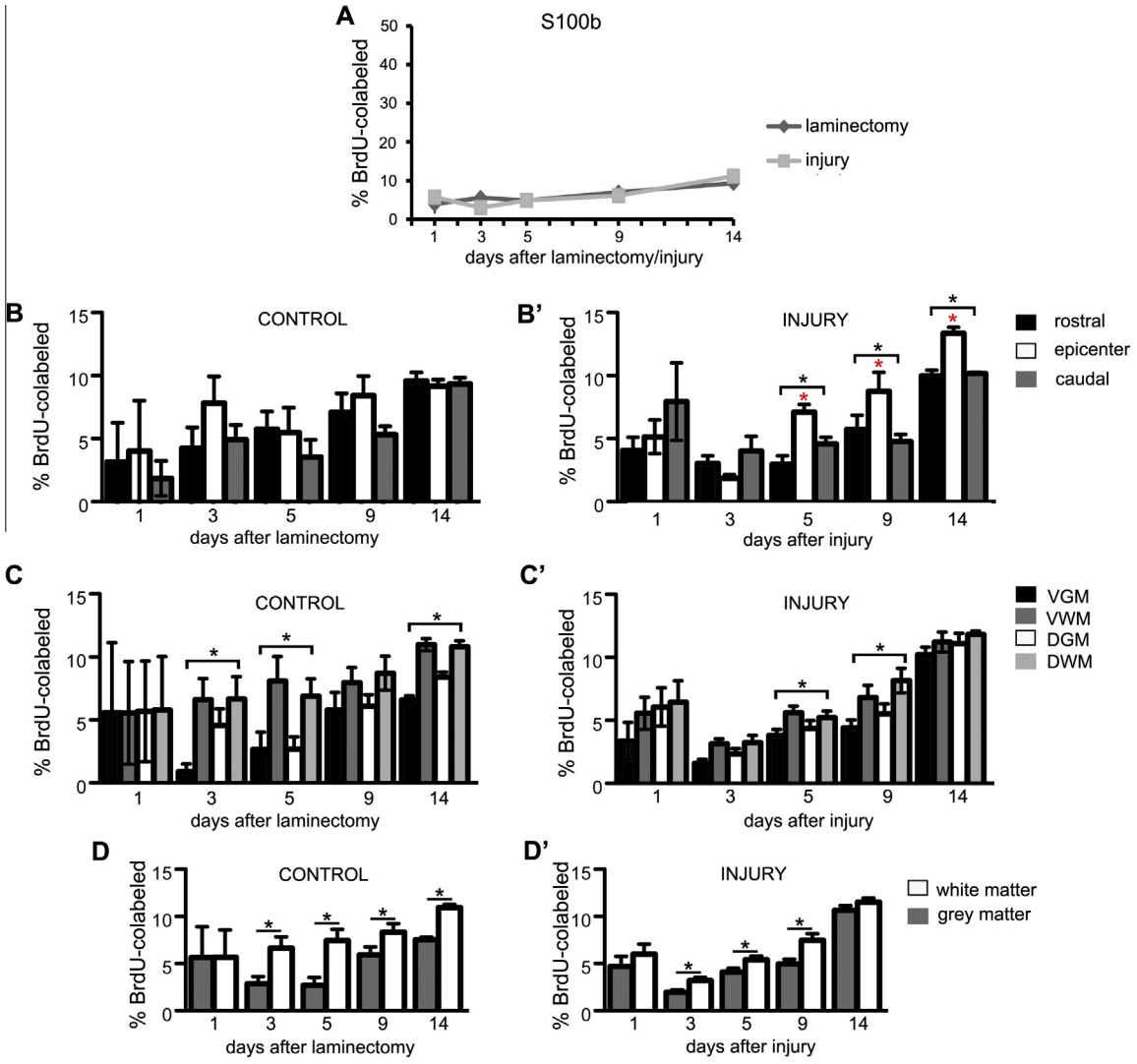

Fig. 9. Proportion of BrdU$^+$ cells colabeling with S100b in control and injured spinal cord. (A) The proportion of BrdU$^+$/S100b$^+$ cells remained relatively unchanged between control and injured tissue. (B) The distribution of BrdU$^+$ cells in different segments of the spinal cord relative to the site of laminectomy was homogeneous in control tissue (p-values > 0.05). (B′) Five days after injury the proportion of double-positive cells increased at the injury epicenter and remained elevated (p-values < 0.05). Bars and black * indicate significance in ANOVA, whereas red * indicates significance in post hoc tests. (C) In control tissue, the proportion of BrdU$^+$/S100b$^+$ cells in the ventral gray matter was significantly lower than all other anatomical areas of the spinal cord (p-values < 0.05). (C′) After injury, the proportion of BrdU$^+$/S100b$^+$ cells in the ventral gray matter was significantly less than some other areas, but not at all time points. Bars and black * indicate significance in ANOVA. (D, D′) More BrdU$^+$/S100b$^+$ cells were present in the white matter than the gray matter in both injured and control spinal cords. (For interpretation of the references to color in this figure legend, the reader is referred to the web version of this article.)

modest decrease from 5.7% ± 1.2% to 3.0% ± 0.48% occurred between 1 and 3 days after injury, and this proportion increased after 5 days to 4.9% ± 0.42%. However, these fluctuations were not statistically significant changes, and they did not significantly vary from the proportions of double-positive cells observed in the control spinal cord at the same time-points (p-values > 0.05).

Five days after injury, there was a difference in the proportion of BrdU$^+$/S100b$^+$ cells between the epicenter and adjacent segments of the spinal cord (p-value < 0.0001), with the epicenter (7.1 ± 0.61%) showing a higher proportion of double-positive cells than the rostral (3.0 ± 0.66%) or caudal (4.6 ± 0.53%) segments (Fig. 9B′). This trend was maintained at 9 and 14 days, but not in the control spinal cord (Fig. 9B). After injury, the proportion of BrdU$^+$/S100b$^+$ cells in the VGM was significantly less than in other regions, but not at all time-points (Fig. 9C). This trend echoed that seen in the control spinal cord (Fig. 9C). After 3 days of BrdU administration, there was a statistically significant difference between the proportions of BrdU$^+$ cells expressing S100b in the white and gray matter, with a higher proportion of BrdU$^+$ co-expressing S100b in the white matter, and this was maintained throughout 14 days (p-values < 0.05; Fig. 9D). Similarly, injured spinal cord displayed this same significant difference and pattern between the white and gray matter,

although the difference between the two regions was lower and not significant 14 days after injury (p-value = 0.1939; Fig. 9D′).

After 1 day of BrdU administration, control spinal cord did not have $BrdU^+/Iba1^+$ cells. $BrdU^+$ cells first expressed Iba1 after 3 days of daily BrdU administration at a proportion of 1.1 ± 0.61% of $BrdU^+$ cells. This proportion increased modestly to 3.5 ± 0.19% after 5 days, and significantly after 9 days to 22.2 ± 2.0% (p-value < 0.0001). After this time-point, the percentage of double-positive cells leveled off in the control spinal cord (p-value > 0.05; Fig. 10A). In contrast to this behavior in the control spinal cord, 1 day after injury the percentage of $BrdU^+/Iba1^+$ cells was 52.4 ± 3.5%. This indicates that $Iba1^+$ microglia/macrophages initiated a very swift proliferative response to injury. After 3 days, the proportion of $BrdU^+/Iba1^+$ cells decreased significantly to 37.1 ± 4.0% (p-value < 0.05), but remained elevated compared with the control spinal cord for the duration of the experiment (p-values < 0.05). In the control spinal cord, the distribution of $BrdU^+/Iba1^+$ cells was homogeneous with regard to rostro-caudal segments (p-values > 0.05; Fig. 10B) and mostly homogenous with regard to dorso-ventral region (p-value < 0.05; Fig. 10C). After injury, the distribution of $BrdU^+/Iba1^+$ cells was mostly homogeneous within the rostro-caudal segments as well. Exceptions to this were an increase in the number

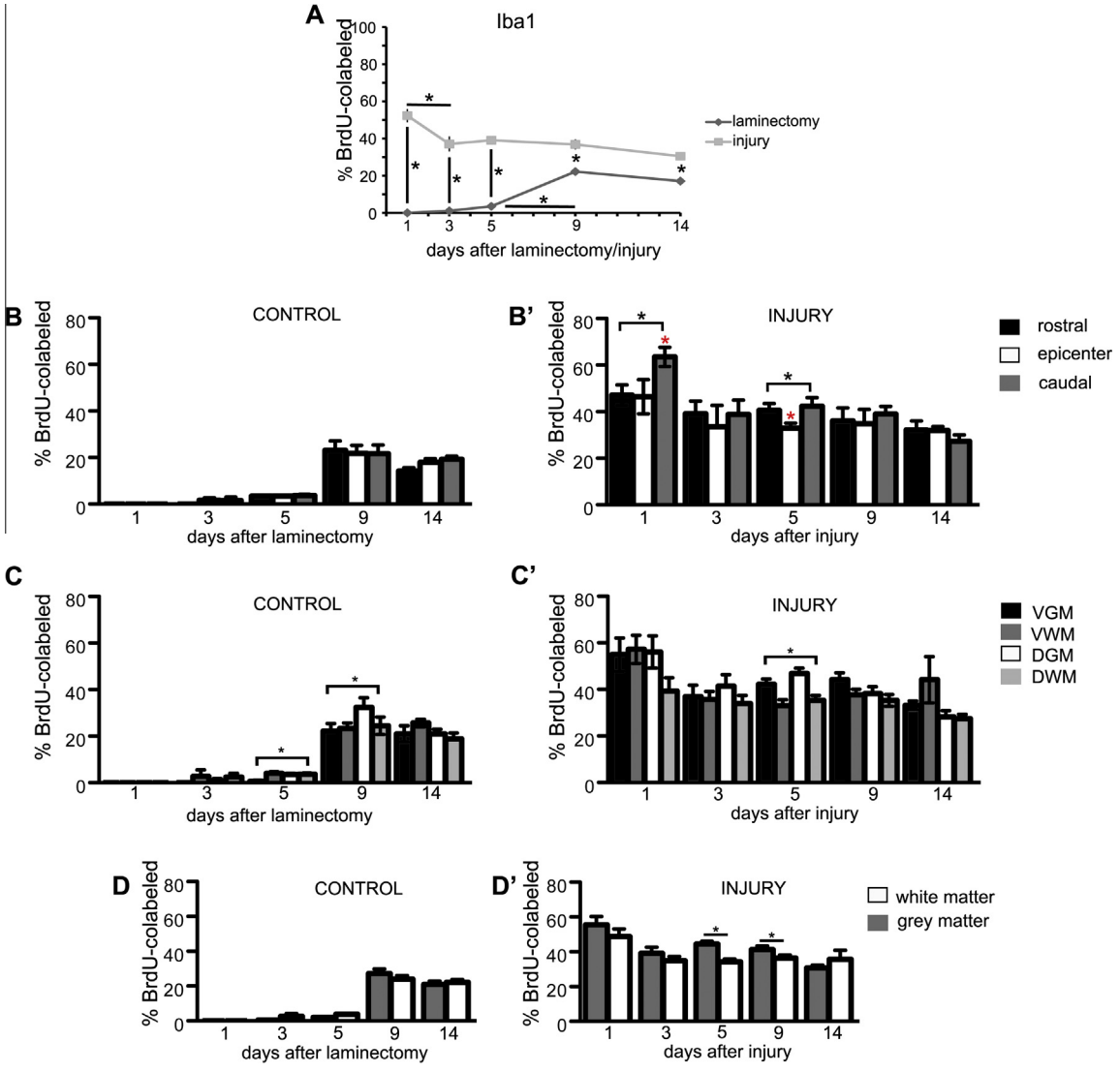

Fig. 10. Proportion of $BrdU^+$ cells colabeling with Iba1 in control and injured spinal cord. (A) Proportion of double-positive cells at all time points and conditions. (B) The proportion of $BrdU^+/Iba1^+$ cells with respect to the location of the laminectomy was homogeneous (p-values > 0.05). (B′) The proportion of $BrdU^+/Iba1^+$ cells with respect to the location of the compression injury varied on days 1 and 5. Bars and black * indicate significance in ANOVA, whereas red * indicates significance in post hoc tests. (C) The proportion of $BrdU^+/Iba1^+$ cells showed near homogeneity across anatomical regions except for the dorsal gray matter after 9 days of BrdU labeling. (C′) The proportion of $BrdU^+/Iba1^+$ cells by anatomical regions after injury showed a preference for the ventral and dorsal gray matter at 5 days after injury. Bars and black * indicate significance in ANOVA. (D, D′) Data from graphs D and E pooled for gray and white matter showed a slight trend toward a higher proportion of $BrdU^+/Iba1^+$ cells after injury, but this did not approach significance. (For interpretation of the references to color in this figure legend, the reader is referred to the web version of this article.)

of BrdU$^+$/Iba1$^+$ cells in the caudal spinal cord 1 day after injury, and a decrease at the epicenter 5 days after injury (p-values < 0.05; Fig. 10B′). One day after injury, the proportion of BrdU$^+$/Iba1$^+$ cells in the DWM was lower than in other regions (p-values < 0.05), while at 3 days this proportion was non-significant across most regions (p-values > 0.05). After 5 days of BrdU administration, both the ventral and DGM in the injured spinal cord had an elevated proportion of double-positive cells compared with the ventral and DWM (p-values < 0.05; Fig. 10C′-9D′). Other than these instances, BrdU$^+$/Iba1$^+$ cells among white and gray matter was homogeneous in the control and in the injured spinal cords (p-values > 0.05; Fig. 10D, D′).

DISCUSSION

The pattern of proliferation and cell fate acquisition was distinct for control and injured spinal cord. In the control spinal cord, the majority of BrdU$^+$ cells expressed the immature glial markers Olig2 or Sox10, while a small number of BrdU$^+$ cells expressed the astrocyte markers S100b and GFAP. This agrees with previously published data showing that the majority of cells proliferating in the uninjured adult spinal cord are glial progenitor cells that primarily differentiate into oligodendrocytes (Horner et al., 2000). There were no BrdU$^+$/Nestin$^+$ or BrdU$^+$/Iba1$^+$ cells present at early time-points in the control spinal cord, and the proportion of BrdU$^+$ cells expressing these markers after multiple days of BrdU administration was low. That these cell types do not appear to proliferate in the uninjured spinal cord until after a few days of BrdU administration indicates that inflammatory processes were not initiated after the laminectomy was performed and instead represent endogenous, baseline levels of proliferation of Nestin$^+$ cells and Iba1$^+$ microglia. These cells have been reported to proliferate at a significantly reduced rate in the intact spinal cord compared with other glial populations (Horner et al., 2000). After injury, the proportion of BrdU$^+$ cells expressing Olig2 or Sox10 decreased drastically, while the proportion of BrdU$^+$ cells expressing Iba1, GFAP, or Nestin increased significantly. Interestingly, the proportion of BrdU$^+$/S100b$^+$ cells changed little after injury. Changes in the proportions of each cell population over time may be a consequence of distinct time-courses of differentiation specific to each cell type, to a temporal loss of marker expression, and/or of temporal changes in the cytokine or trophic factor profile of the post-injury spinal cord (Sellers and Horner, 2005; Stammers et al., 2012).

Our findings agree with those published for contusion models, which feature a distinct distribution of cell types between the injury epicenter and surrounding spinal segments. In our study, the cell fate of BrdU$^+$ cells often varied between the lesion epicenter and adjacent rostro-caudal segments of the spinal cord, and between the various dorso-ventral regions. In previously published studies on contusion injuries, macrophages were the predominant dividing cell type within the lesion and the majority of dividing cells in surrounding tissues were Ng2$^+$ glial precursor cells, followed by oligodendrocytes and astrocytes (Zai and Wrathall, 2005; Lytle and Wrathall, 2007). Similarly, Nestin$^+$ and GFAP$^+$ cells were upregulated in response to contusive injury (Takahashi et al., 2003). These previous reports on responses to contusive injury match our findings for the lateral compression model of SCI. We observed an initial increase in the proportion of BrdU$^+$ cells expressing Nestin, GFAP, or Iba1 as early as 1 day after injury and these populations fluctuated independently over time, but generally began to decrease as the study progressed into later time-points. Additionally, our data indicate that the greatest proliferation after a compression injury occurs 3 days after injury, with a larger proliferative response at the injury epicenter. This agrees with previously published time-courses of cellular proliferation in contusion models of SCI (Namiki and Tator, 1999; McTigue et al., 2001; Zai and Wrathall, 2005; Lytle and Wrathall, 2007). In comparison with another study examining cellular proliferation and neuroprogenitor cell response to compressive SCI (Ke et al., 2006), we found no evidence for neuronogenesis after compressive injury. If neuronogenesis is occurring after injury, it may be occurring in cells that did not enter S-phase, and thus was not observed in our study.

In the control spinal cord, we observed fewer BrdU$^+$ cells in the VGM than in the other anatomical regions. This may be due to differences in area between the VGM and the other spinal cord regions, particularly the extensive VWM. However, we observed that after injury, there were similar numbers of BrdU$^+$ cells in the VGM as in other regions of the spinal cord, and that the average number of BrdU$^+$ cells per slice in the VGM was often not statistically significant compared with other regions, particularly at later time-points after injury. Prior work indicates that in the intact spinal cord, proliferation most frequently occurs along the outer circumference of the spinal cord (Horner et al., 2000), which excludes the VGM and includes all other regions of interest in our study. Our finding that at early time-points after injury, but not at later time-points, there is a statistically significant difference in the number of BrdU$^+$ cells between the VGM and VWM, may be due to an increased rate of mitosis of precursor cells in the subpial white matter and to further rounds of mitosis after migration and arrival at the ventral horn.

Numerous studies have demonstrated that ependymal cells of the spinal cord rapidly proliferate in response to various models of SCI and disease (Vaquero et al., 1987; Beattie et al., 1997; Takahashi et al., 2003; Danilov et al., 2006; Horky et al., 2006; Ke et al., 2006; Tu et al., 2010; McDonough and Martinez-Cerdeno, 2012). We find a discrepancy between the total number and the fold increases in cell division at the CC between our model and those reported in other SCI models. We hypothesize that the discrepancy between our data and the data from other studies is due to an injury type specific proliferative response of the ependymal cells. For instance, a lateral compressive force or incision would trigger low levels of ependymal

proliferation (Takahashi et al., 2003), but a direct injury of the ependymal cell processes by a dorsal contusive force or dorsal incision would generate a more robust mitotic response of the ependymal cells (Johansson et al., 1999). This has been suggested in another study, which compared ependymal proliferation after an incision in different regions of the spinal cord; the dorsal funiculus incision injury resulted in a greater increase in ependymal cell proliferation than a lateral incision injury (Meletis et al., 2008). Admittedly, our model only accounts for the $BrdU^+$ cells currently located within the CC at the time of perfusion and analysis. With our method, we cannot differentiate between mitotic cells located near the ependymal layer in the gray matter and cells that were born at the CC and migrated outward into the gray matter.

It is generally agreed that the rat response is more similar to humans after SCI than mice. For example, neither rats nor humans will regain the ability to void their bladder voluntarily after injury (Lee et al., 2013), but mice are capable of recovering micturition (Plemel et al., 2008). Furthermore, rats develop a cavity after SCI that resembles syringomyelia in humans (Basso et al., 1996; Beattie et al., 1997), whereas injury in mice typically results in a fibrous lesion (Zhang et al., 1996; Jakeman et al., 2000; Inman et al., 2002; Plemel et al., 2008; Piltti et al., 2013). Despite these pathological differences, the Wrathall group has published papers on the proliferative response to contusive SCI in both mouse and rat which indicate that the proliferative response is largely conserved between the two species (Zai and Wrathall, 2005; Lytle and Wrathall, 2007).

Our data provide further insight into the dynamics of cell fate marker expression after SCI. We demonstrate that after injury there are marked differences in the fate of the newly generated cells between dorso-ventral regions and rostro-caudal segments, and also over time. This is in contrast to our observations in the control spinal cord, which indicate that the proportion of cells expressing specific markers changes little along the rostro-caudal or dorso-ventral axes. These data should be a consideration in the development of transplantation therapies. Data from other groups agree that the microenvironment of the spinal cord after injury influences cell fate, at least of transplanted cells (Nakamura et al., 2003; Nishimura et al., 2013), which may also have an effect on endogenous proliferating cells in the spinal cord. These same studies indicate that the inflammatory responses are greatest at early time points and begin to subside after one to two weeks. As our data show, the compression injury epicenter elicits a large proliferative response of cells expressing microglial/macrophage markers, and this persists through the first 14 days of injury. Furthermore, stem cell transplantations were more successful when cells were administered 9 days after injury (Parr et al., 2007; Tarasenko et al., 2007; Li et al., 2011; Piltti et al., 2013). The choice of this time point was chosen based on other studies indicating a reduced inflammatory response, which may signify a more permissive environment for stem cells to survive in (Nakamura et al., 2003; Nishimura et al., 2013). At this time-point our data indicate that the rate of proliferation in endogenous progenitors has slowed to near control levels and the number of newly generated cells expressing Nestin or GFAP has decreased, although the proportion of $BrdU^+/Iba1^+$ cells remained elevated relative to the control spinal cord.

Our finding that the fate of proliferative cells varies among dorso-ventral regions and over time indicates a need for further research into the patterns of cytokine and pro-inflammatory molecule expression after injury within discrete regions of the spinal cord, particularly the white and gray matter. Furthermore, our data imply that regenerative therapies may not be applicable to the entire spinal cord because of variations in the extracellular environment in the gray matter and in the white matter; one cocktail of cytokines and transcription factors may be needed to modulate cell differentiation in the gray matter, but an entirely different combination may be necessary to modulate the environment of the white matter. Our data also indicate that the Plemel SCI model of calibrated forceps compression (Plemel et al., 2008) generates a very similar phenotype to published models of contusion injury generated using other methods.

Acknowledgements—Financial support for this study was provided by the Shriners Hospitals for Children and a training grant fellowship awarded by the California Institute for Regenerative Medicine (CIRM). The authors have no competing interests to declare.

REFERENCES

Barnabe-Heider F, Goritz C, Sabelstrom H, Takebayashi H, Pfrieger FW, Meletis K, Frisen J (2010) Origin of new glial cells in intact and injured adult spinal cord. Cell Stem Cell 7:470–482.

Basso DM, Beattie MS, Bresnahan JC (1996) Graded histological and locomotor outcomes after spinal cord contusion using the NYU weight-drop device versus transection. Exp Neurol 139:244–256.

Beattie MS, Bresnahan JC, Komon J, Tovar CA, Van Meter M, Anderson DK, Faden AI, Hsu CY, Noble LJ, Salzman S, Young W (1997) Endogenous repair after spinal cord contusion injuries in the rat. Exp Neurol 148:453–463.

Chaplan SR, Bach FW, Pogrel JW, Chung JM, Yaksh TL (1994) Quantitative assessment of tactile allodynia in the rat paw. J Neurosci Methods 53:55–63.

Chen C, Daugherty D, Jiang P, Deng W (2012) Oligodendrocyte progenitor cells derived from mouse embryonic stem cells give rise to type-1 and type-2 astrocytes in vitro. Neurosci Lett 523:180–185.

Danilov AI, Covacu R, Moe MC, Langmoen IA, Johansson CB, Olsson T, Brundin L (2006) Neurogenesis in the adult spinal cord in an experimental model of multiple sclerosis. Eur J Neurosci 23:394–400.

Eftekharpour E, Karimi-Abdolrezaee S, Fehlings MG (2008) Current status of experimental cell replacement approaches to spinal cord injury. Neurosurg Focus 24:E19.

Fouad K, Klusman I, Schwab ME (2004) Regenerating corticospinal fibers in the Marmoset (*Callitrix jacchus*) after spinal cord lesion and treatment with the anti-Nogo-A antibody IN-1. Eur J Neurosci 20:2479–2482.

Gensel JC, Tovar CA, Hamers FP, Deibert RJ, Beattie MS, Bresnahan JC (2006) Behavioral and histological characterization of unilateral cervical spinal cord contusion injury in rats. J Neurotrauma 23:36–54.

Glass JD, Boulis NM, Johe K, Rutkove SB, Federici T, Polak M, Kelly C, Feldman EL (2012) Lumbar intraspinal injection of neural stem cells in patients with amyotrophic lateral sclerosis: results of a phase I trial in 12 patients. Stem Cells 30:1144–1151.

Grossman SD, Rosenberg LJ, Wrathall JR (2001) Temporal–spatial pattern of acute neuronal and glial loss after spinal cord contusion. Exp Neurol 168:273–282.

Hawryluk GW, Rowland J, Kwon BK, Fehlings MG (2008) Protection and repair of the injured spinal cord: a review of completed, ongoing, and planned clinical trials for acute spinal cord injury. Neurosurg Focus 25:E14.

Horky LL, Galimi F, Gage FH, Horner PJ (2006) Fate of endogenous stem/progenitor cells following spinal cord injury. J Comp Neurol 498:525–538.

Horner PJ, Power AE, Kempermann G, Kuhn HG, Palmer TD, Winkler J, Thal LJ, Gage FH (2000) Proliferation and differentiation of progenitor cells throughout the intact adult rat spinal cord. J Neurosci 20:2218–2228.

Inman D, Guth L, Steward O (2002) Genetic influences on secondary degeneration and wound healing following spinal cord injury in various strains of mice. J Comp Neurol 451:225–235.

Jakeman LB, Guan Z, Wei P, Ponnappan R, Dzwonczyk R, Popovich PG, Stokes BT (2000) Traumatic spinal cord injury produced by controlled contusion in mouse. J Neurotrauma 17:299–319.

Johansson CB, Momma S, Clarke DL, Risling M, Lendahl U, Frisen J (1999) Identification of a neural stem cell in the adult mammalian central nervous system. Cell 96:25–34.

Karussis D, Karageorgiou C, Vaknin-Dembinsky A, Gowda-Kurkalli B, Gomori JM, Kassis I, Bulte JW, Petrou P, Ben-Hur T, Abramsky O, Slavin S (2010) Safety and immunological effects of mesenchymal stem cell transplantation in patients with multiple sclerosis and amyotrophic lateral sclerosis. Arch Neurol 67:1187–1194.

Ke Y, Chi L, Xu R, Luo C, Gozal D, Liu R (2006) Early response of endogenous adult neural progenitor cells to acute spinal cord injury in mice. Stem Cells 24:1011–1019.

Lee YS, Lin CY, Jiang HH, Depaul M, Lin VW, Silver J (2013) Nerve regeneration restores supraspinal control of bladder function after complete spinal cord injury. J Neurosci 33:10591–10606.

Li Y, Zhang WM, Wang TH (2011) Optimal location and time for neural stem cell transplantation into transected rat spinal cord. Cell Mol Neurobiol 31:407–414.

Liebscher T, Schnell L, Schnell D, Scholl J, Schneider R, Gullo M, Fouad K, Mir A, Rausch M, Kindler D, Hamers FP, Schwab ME (2005) Nogo-A antibody improves regeneration and locomotion of spinal cord-injured rats. Ann Neurol 58:706–719.

Lytle JM, Wrathall JR (2007) Glial cell loss, proliferation and replacement in the contused murine spinal cord. Eur J Neurosci 25:1711–1724.

Marques SA, Garcez VF, Del Bel EA, Martinez AM (2009) A simple, inexpensive and easily reproducible model of spinal cord injury in mice: morphological and functional assessment. J Neurosci Methods 177:183–193.

Mazzini L, Ferrero I, Luparello V, Rustichelli D, Gunetti M, Mareschi K, Testa L, Stecco A, Tarletti R, Miglioretti M, Fava E, Nasuelli N, Cisari C, Massara M, Vercelli R, Oggioni GD, Carriero A, Cantello R, Monaco F, Fagioli F (2010) Mesenchymal stem cell transplantation in amyotrophic lateral sclerosis: a phase I clinical trial. Exp Neurol 223:229–237.

McDonough A, Martinez-Cerdeno V (2012) Endogenous proliferation after spinal cord injury in animal models. Stem Cells Int 2012:387513.

McTigue DM, Wei P, Stokes BT (2001) Proliferation of NG2-positive cells and altered oligodendrocyte numbers in the contused rat spinal cord. J Neurosci 21:3392–3400.

Meletis K, Barnabe-Heider F, Carlen M, Evergren E, Tomilin N, Shupliakov O, Frisen J (2008) Spinal cord injury reveals multilineage differentiation of ependymal cells. PLoS Biol 6:e182.

Menet V, Prieto M, Privat A, Gimenez y Ribotta M (2003) Axonal plasticity and functional recovery after spinal cord injury in mice deficient in both glial fibrillary acidic protein and vimentin genes. Proc Natl Acad Sci U S A 100:8999–9004.

Mothe AJ, Tator CH (2005) Proliferation, migration, and differentiation of endogenous ependymal region stem/progenitor cells following minimal spinal cord injury in the adult rat. Neuroscience 131:177–187.

Nakamura M, Houghtling RA, MacArthur L, Bayer BM, Bregman BS (2003) Differences in cytokine gene expression profile between acute and secondary injury in adult rat spinal cord. Exp Neurol 184:313–325.

Namiki J, Tator CH (1999) Cell proliferation and nestin expression in the ependyma of the adult rat spinal cord after injury. J Neuropathol Exp Neurol 58:489–498.

Nishimura S, Yasuda A, Iwai H, Takano M, Kobayashi Y, Nori S, Tsuji O, Fujiyoshi K, Ebise H, Toyama Y, Okano H, Nakamura M (2013) Time-dependent changes in the microenvironment of injured spinal cord affects the therapeutic potential of neural stem cell transplantation for spinal cord injury. Mol Brain 6:3.

Okano H, Sakaguchi M, Ohki K, Suzuki N, Sawamoto K (2007) Regeneration of the central nervous system using endogenous repair mechanisms. J Neurochem 102:1459–1465.

Parr AM, Kulbatski I, Tator CH (2007) Transplantation of adult rat spinal cord stem/progenitor cells for spinal cord injury. J Neurotrauma 24:835–845.

Petit A, Sanders AD, Kennedy TE, Tetzlaff W, Glattfelder KJ, Dalley RA, Puchalski RB, Jones AR, Roskams AJ (2011) Adult spinal cord radial glia display a unique progenitor phenotype. PLoS ONE 6:e24538.

Piltti KM, Salazar DL, Uchida N, Cummings BJ, Anderson AJ (2013) Safety of epicenter versus intact parenchyma as a transplantation site for human neural stem cells for spinal cord injury therapy. Stem Cells Transl Med 2:204–216.

Plemel JR, Duncan G, Chen KW, Shannon C, Park S, Sparling JS, Tetzlaff W (2008) A graded forceps crush spinal cord injury model in mice. J Neurotrauma 25:350–370.

Ruff RL, McKerracher L, Selzer ME (2008) Repair and neurorehabilitation strategies for spinal cord injury. Ann N Y Acad Sci 1142:1–20.

Sellers DL, Horner PJ (2005) Instructive niches: environmental instructions that confound NG2 proteoglycan expression and the fate-restriction of CNS progenitors. J Anat 207:727–734.

Sellers DL, Maris DO, Horner PJ (2009) Postinjury niches induce temporal shifts in progenitor fates to direct lesion repair after spinal cord injury. J Neurosci 29:6722–6733.

Stammers AT, Liu J, Kwon BK (2012) Expression of inflammatory cytokines following acute spinal cord injury in a rodent model. J Neurosci Res 90:782–790.

Takahashi M, Arai Y, Kurosawa H, Sueyoshi N, Shirai S (2003) Ependymal cell reactions in spinal cord segments after compression injury in adult rat. J Neuropathol Exp Neurol 62:185–194.

Tarasenko YI, Gao J, Nie L, Johnson KM, Grady JJ, Hulsebosch CE, McAdoo DJ, Wu P (2007) Human fetal neural stem cells grafted into contusion-injured rat spinal cords improve behavior. J Neurosci Res 85:47–57.

Tu J, Liao J, Stoodley MA, Cunningham AM (2010) Differentiation of endogenous progenitors in an animal model of post-traumatic syringomyelia. Spine 35:1116–1121 (Phila Pa 1976).

Vaquero J, Ramiro MJ, Oya S, Cabezudo JM (1981) Ependymal reaction after experimental spinal cord injury. Acta Neurochir (Wien) 55:295–302.

Vaquero J, Ramiro MJ, Oya S, Cabezudo JM (1987) Ependymal cell proliferation after spinal cord injury. Surg Neurol 28:401.

Watson C, Paxinos G, Kayalioglu G (2009) The spinal cord: a Christopher and Dana Reeve foundation text and atlas. Elsevier Science.

Weidner N, Ner A, Salimi N, Tuszynski MH (2001) Spontaneous corticospinal axonal plasticity and functional recovery after adult central nervous system injury. Proc Natl Acad Sci U S A 98:3513–3518.

Zai LJ, Wrathall JR (2005) Cell proliferation and replacement following contusive spinal cord injury. Glia 50:247–257.

Zai LJ, Yoo S, Wrathall JR (2005) Increased growth factor expression and cell proliferation after contusive spinal cord injury. Brain Res 1052:147–155.

Zhang Z, Fujiki M, Guth L, Steward O (1996) Genetic influences on cellular reactions to spinal cord injury: a wound-healing response present in normal mice is impaired in mice carrying a mutation (WldS) that causes delayed Wallerian degeneration. J Comp Neurol 371:485–495.

(Accepted 4 September 2013)
(Available online 14 September 2013)